

MULTIPLICITY OF THE GALACTIC SENIOR CITIZENS: A HIGH-RESOLUTION SEARCH FOR COOL SUBDWARF COMPANIONS

CARL ZIEGLER¹, NICHOLAS M. LAW¹, CHRISTOPH BARANEC², REED L. RIDDLE³, AND JOSHUA T. FUCHS¹

Submitted to ApJ

ABSTRACT

Cool subdwarfs are the oldest members of the low-mass stellar population. Mostly present in the galactic halo, subdwarfs are characterized by their low-metallicity. Measuring their binary fraction and comparing it to solar-metallicity stars could give key insights into the star formation process early in the Milky Way's history. However, because of their low luminosity and relative rarity in the solar neighborhood, binarity surveys of cool subdwarfs have suffered from small sample sizes and incompleteness. Previous surveys have suggested that the binary fraction of red subdwarfs is much lower than for their main-sequence cousins. Using the highly efficient Robo-AO system, we present the largest yet high-resolution survey of subdwarfs, sensitive to angular separations ($\rho \geq 0''.15$) and contrast ratios ($\Delta m_i \leq 6$) invisible in past surveys. Of 344 target cool subdwarfs, 40 are in multiple systems, 16 newly discovered, for a binary fraction of $11.6\% \pm 1.8\%$. We also discovered 6 triple star systems for a triplet fraction of $1.7\% \pm 0.7\%$. Comparisons to similar surveys of solar-metallicity dwarf stars gives a $\sim 3\sigma$ disparity in luminosity between companion stars, with subdwarfs displaying a shortage of low-contrast companions. We also observe a lack of close subdwarf companions in comparison to similar-mass dwarf multiple systems.

Subject headings: binaries: close - subdwarfs - stars: late-type - instrumentation: adaptive optics - techniques: high angular resolution - methods: data analysis

1. INTRODUCTION

Cool subdwarfs are the oldest members of the low-mass stellar population, with spectral types of K and M, masses between ~ 0.6 and $\sim 0.08 M_{\odot}$, and surface effective temperatures between 4000 and 2300 K (Kaltenegger et al. 2009). First coined by Kuiper (1939), subdwarfs are the low-luminosity, metal-poor ($[Fe/H] < -1$) spectral counterparts to the main sequence dwarfs. On a color-magnitude diagram, subdwarfs lie between white dwarfs and the main sequence (Adams 1915). With decreased metal opacity, subdwarfs have smaller stellar radii and are bluer at a given luminosity than their main sequence counterparts (Sandage & Eggen 1959). These low-mass stars are members of the Galactic halo and have higher systematic velocities and proper motions than disk dwarf stars. Traditionally subdwarfs have been identified using high proper motion surveys. Although 99.7% of stars in the galaxy are disk main sequence, statistically there are more subdwarfs in these high PM surveys (Reid & Hawley 2005).

The search for companions to stars of different masses gives clues to the star formation process, as any successful model must account for both the frequency of the multiple star systems and the properties of the systems. In addition, monitoring the orbital characteristics of multiple star systems yields information otherwise unattainable for single stars, such as relative brightness and masses of the components (Goodwin et al. 2007), lending further constraints to mass-luminosity relationships (Chabrier et al. 2000)

Old population II stars are important probes for the early history of star formation in the galaxy (Zhang et al.

2013). The formation process of low mass stars remains less well understood than for solar-like stars. Although multiple indications suggest they form as the low-mass tail of regular star formation (Bourke et al. 2006), other mechanisms have been proposed for some or all of these objects (Goodwin & Whitworth 2007; Thies & Kroupa 2007; Basu & Vorobyov 2012). A firm binary fraction for low-metallicity cool stars could assist in constraining various formation models. This again motivates the need for a comprehensive binarity survey, sensitive to small angular separations.

The multiplicity of main sequence dwarfs has been well explored in the literature. A consistent trend that has pervaded is that the percentage of stars with stellar companions seems to depend on the mass of the stars. For AB-type stars, Peter et al. (2012) used a sample of 148 stars to determine a companion fraction of $\sim 70\%$. For solar type stars (FGK-type), around 57% have companions (Duquennoy & Mayor 1991), although Raghavan et al. (2010) have revised the fraction down to $\sim 46\%$. Fischer and Marcy (1992) looked at M-dwarfs and found a multiplicity fraction of $42 \pm 9\%$. More recently, Janson et al. (2012) find a binary fraction for late K- to mid M-type dwarfs of $27 \pm 3\%$ from a sample of 701 stars. For late M-dwarfs, a slightly lower fraction was found by Law et al. (2006b) of $7 \pm 3\%$. Extending their previous study for mid/late M-type dwarfs, M5-M8, Janson et al. (2014) find a multiplicity fraction of 21%-27% using a sample of 205 stars.

While the multiplicity of dwarf stars has been heavily studied with comprehensive surveys, detailed multiplicity studies of low-mass subdwarfs have, historically, been hindered by their low luminosities and relative rarity in the solar neighborhood. Within 10 pc, there are three low-mass subdwarfs, compared to 243 main sequence stars (Monteiro et al. 2006). Subsequently, multiplicity surveys of cool subdwarfs have been relatively small. The largest, a low-limit angular resolution search by Zhang et al. (2013) mined the Sloan Digital

carlziegler@unc.edu

¹ Department of Physics and Astronomy, University of North Carolina at Chapel Hill, Chapel Hill, NC 27599-3255, USA

² Institute for Astronomy, University of Hawai'i at Mānoa, HI 96720-2700, USA

³ Division of Physics, Mathematics, and Astronomy, California Institute of Technology, Pasadena, CA, 91125, USA

Table 1 The specifications of the Robo-AO subdwarf survey

Filter	Sloan i' -band
FWHM resolution	$0'.15$
Field size	$44'' \times 44''$
Detector format	1024^2 pixels
Pixel scale	43.1 mas / pix
Exposure time	120 seconds
Subdwarf targets	344
Targets observed / hour	20
Observation dates	September 1 2012 – August 21 2013

Sky Survey (York et al. 2000) to find 1826 cool subdwarfs, picking out subdwarfs by their PMs and identifying spectral type by fitting an absolute magnitude-spectral type relationship. They find 45 subdwarfs multiple systems in total, with 30 being wide companions and 15 partially resolved companions. When adjusting for the incompleteness of their survey, an estimate of the binary fraction of $>10\%$ is predicted. The authors note the need for a high spatial resolution imaging survey to search for close binaries (<100 AU) and put tighter constraints on the binary fraction of cool subdwarfs.

The high-resolution subdwarf surveys completed thus far have been comparatively small. Gizis & Reid (2000) detected no companions in a sample of eleven cool subdwarfs. Riaz et al. (2008) similarly found no companions in a sample of nineteen M subdwarfs using the *Hubble Space Telescope*. Lodieu et al. (2009) reported one companion in a sample of 33 M type subdwarfs. Jao et al. (2009) found four companions in a sample of 62 cool subdwarf systems. With the high variance in small number statistics, the relationship between dwarf and subdwarf multiplicity fractions remains inconclusive.

We present here the largest high resolution cool subdwarf multiplicity survey yet performed, making use of the efficient Robo-AO system. The Robo-AO system allows us to detect more cool and close companion stars in a much larger sample size than previously possible. This survey combines previously known wide proper-motion pairs, spectroscopic binaries, and high angular resolution images able to detect companions with $\rho \geq 0'.15$ and $\Delta m_i \leq 6$.

The paper is organized as follows. In Section 2 we describe the target selection, the Robo-AO system, and follow-up observations. In Section 3 we describe the Robo-AO data reduction and the companion detection and analysis. In Section 4 we describe the results of this survey, including discovered companions, and compare to similar dwarf surveys. The results are discussed in Section 5 and put in context of previous literature. We conclude in Section 6.

2. SURVEY TARGETS AND OBSERVATIONS

2.1. Sample Selection

We selected targets from the 564 spectral type F- through M-subdwarfs studied by Marshall (2007). These targets were selected from the New Luyten Two-Tenths (NLTT) catalog (Luyten 1979; Luyten & Hughes 1980) of high proper motion stars (>0.18 arcsec/year) using a reduced proper motion diagram (RPM). To distinguish subdwarf stars from their solar-metallicity companions on the main sequence, the RPM used a $(V - J)$ optical-infrared baseline, a technique first used by Salim & Gould (2002), rather than the shorter $(B - R)$ baseline

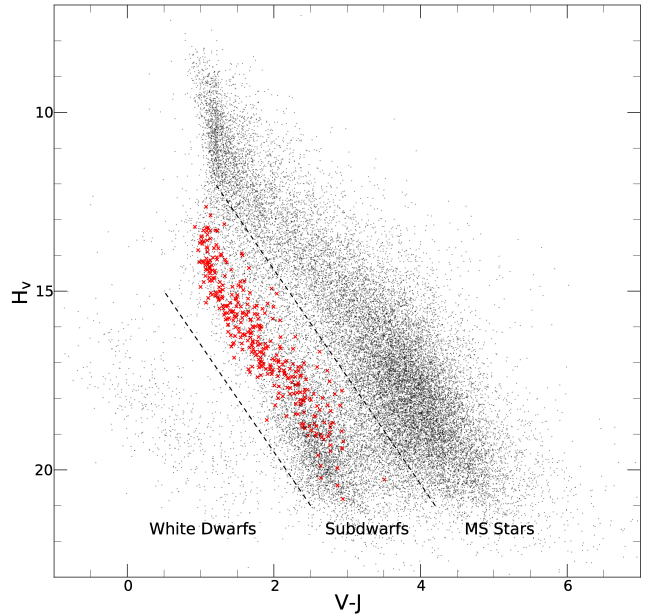


Figure 1. Reduced proper motion diagram of the complete rNLTT (Gould & Salim 2003), with our observed subdwarfs in red X's. The discriminator lines between solar-metallicity dwarfs, metal-poor subdwarfs, and white dwarfs are at $\eta = 0$ and 5.15 , respectively, and with $b = \pm 30$. The subdwarfs plotted make use of the improved photometry of Marshall (2007).

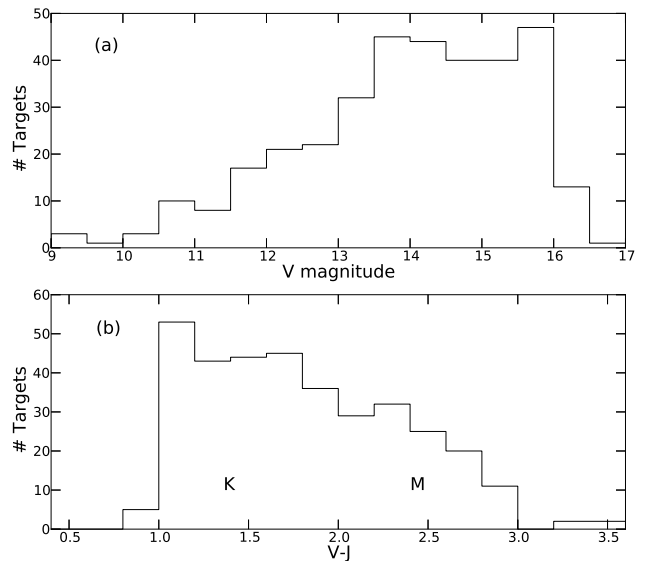


Figure 2. (a) Histogram of magnitudes in V band of the 348 observed subdwarfs. (b) Histogram of the $(V - J)$ colors of the observed subdwarf sample, with approximate spectral types regions K and M marked. Both plots use the photometry of Marshall (2007)

used by Luyten. This method uses the high proper motion as a proxy for distance and the blueness of subdwarfs relative to equal luminosity dwarf stars to separate out main sequence members of the local disk and the halo subdwarfs (Marshall 2008). The reduced proper motion, H_M , is defined as

$$H_M = m + 5 \log \mu + 5 \quad (1)$$

where m is the apparent magnitude and μ is the proper motion in $''/\text{yr}$. The discriminator, η , developed by Salim & Gould to

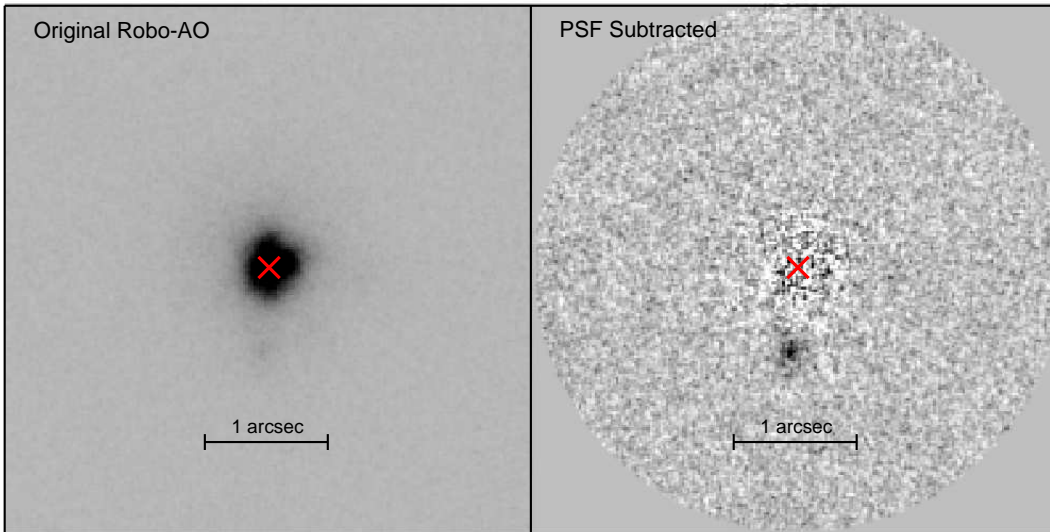


Figure 3. Example of PSF subtraction on NLTT31240 with companion separation of $0''.74$. The red X marks the position of the primary star’s PSF peak. Successful removal of PSF leaves residuals consistent with photon noise.

separate luminosity classes, is defined as

$$\eta(H_V, V - J, \sin b) = H_V - 3.1(V - J) - 1.47|\sin b| - 7.73 \quad (2)$$

where b is the Galactic latitude. The reduced proper motion diagram for the revised NLTT (rNLTT) catalog (Gould & Salim 2003) and our subdwarf targets is presented in Figure 1. The improved photometry of Marshall (2007) placed 12 of the original suspected subdwarfs outside the subdwarf sequence. These stars were rejected from our sample. Of the 552 subdwarfs confirmed by Marshall, a randomly-selected sample of 348 K- and M-subdwarfs were observed by Robo-AO when available between other high priority surveys. The V-band magnitudes and $(V - J)$ colors of the observed subdwarf sample are shown in Figure 2.

2.2. Observations

2.2.1. Robo-AO

We obtained high-angular-resolution images of the 348 subdwarfs during 32 separate nights of observations between 2012 September 3 and 2013 August 21 (UT). The observations were performed using the Robo-AO laser adaptive optics system (Baranec et al. 2013, 2014; Riddle et al. 2012) mounted on the Palomar 60 inch telescope. The first robotic laser guide star adaptive optics system, the automatic Robo-AO system can efficiently observe large, high-resolution surveys. All images were taken using the Sloan i' -band filter (York et al. 2000) and with exposure times of 120 s. Typical seeing at the Palomar Observatory is between $0''.8$ and $1''.8$, with median around $1''.1$ (Baranec et al. 2014). The typical FWHM (diffraction limited) resolution of the Robo-AO system is $0''.12$ - $0''.15$. Specifications of the Robo-AO system are summarized in Table 1.

The images were reduced by the Robo-AO imaging pipeline described in Law et al. (2006a,b, 2009, 2014). The EMCCD frames are dark-subtracted and flat-fielded and then, using the Drizzle algorithm (Fruchter & Hook 2002), stacked and aligned, while correcting for image motion using a bright star in the field. The algorithm also introduces a factor-of-two up-sampling to the images. Since the subdwarf targets are in relatively sparse stellar fields, for the majority of the images the only star visible is the target star and was thus used to correct for the image motion.

2.2.2. Keck LGS-AO

Six candidate multiple systems were selected for re-imaging by the NIRC2 camera behind the Keck II laser guide star adaptive optics system (Wizinowich et al. 2006; van Dam et al. 2006), located in Maunakea, Hawaii, on 2014 August 17 (UT) to confirm possible companions. The targets were selected for their low significance of detectability, either because of low contrast ratio or small angular separation. The observations were done in the K' and H bands with three 90 s exposures for two targets and three 30 s for five targets in a 3-position dither pattern that avoided the noisy, lower-left quadrant. We used the narrow camera setting ($0''.0099/\text{px}$), which gave a single-frame field of view of $10'' \times 10''$.

2.2.3. SOAR Goodman Spectroscopy

We took spectra of 24 of the subdwarfs using the Southern Astrophysical Research Telescope and the Goodman Spectrograph (Clemens et al. 2004) on 2014 July 15. We observed twelve targets with companions and twelve single stars as reference. The spectra were taken using a 930 lines/mm grating with $0.42 \text{ \AA}/\text{pixel}$, a $1''.07$ slit, and exposure times of 480 s.

3. DATA REDUCTION AND ANALYSIS

3.1. Robo-AO Imaging

3.1.1. Target Verification

To verify that each star viewed in the image is the desired subdwarf target, we created Digital Sky Survey cutouts of similar angular size around the target coordinates. Each image was then manually checked to assure no ambiguity in the target star. The vast majority of the targets are in relatively sparse stellar regions. Four of the target stars in crowded fields whose identification was ambiguous were discarded, leaving 344 verified subdwarf targets.

3.1.2. PSF Subtraction

To locate close companions, a custom locally optimized point spread function (PSF) subtraction routine (Law et al. 2014) based on the Locally Optimized combination of Images algorithm (Lafrenière et al. 2007) was applied to centered cutouts of all stars. Other subdwarf observations taken at similar times were used as references, as it is unlikely to

have a companion found in the same position for two different targets. For each target image and for 20 reference images selected as the closest to the target image in observation time, the region around the star was subdivided into polar sections, five up-sampled pixels in radius and 45° in angle. A locally optimized estimate of the PSF for each section was then generated using a linear combination of the reference PSFs. The algorithm begins with an average over the reference PSFs, then uses a downhill simplex algorithm to optimize the contributions from each reference image to find the best fit to the target image. The optimization is done on several coincident sections simultaneously to minimize the probability of subtracting out a real companion, with only the central region outputted to the final PSF. This also provides smoother transitions between adjacent sections as many of the image pixels were shared in the optimization.

After iterating over all sections of the image, the final PSF is an optimal local combination of all the reference PSFs. This final PSF is then subtracted from the original reference image, leaving residuals that are consistent with photon noise. Figure 3 shows an example of the PSF subtraction performance.

We manually checked the final subtracted images for close companions detections ($>5\sigma$). The initial search was limited to a detection radius of $1''$ from the target star. We subsequently performed a secondary search out to a radius of $2''$.

3.1.3. Imaging Performance Metrics

The two dominant factors that effect the image performance of the Robo-AO system are seeing and target brightness. To further classify the image performance for each target an automated routine was ran on all images. Described in detail in Law et al. (2014), the code uses two Moffat functions fit to the PSF to separate the widths of the core and halo. We found that the core size was an excellent predictor of the contrast performance, and used it to group targets into three levels (low, medium and high). Counter-intuitively, the PSF core size decreases as image quality decreases. This is caused by poor S/N on the shift-and-add image alignment used by the EMCCD detector. The frame alignment subsequently locks onto photo noise spikes, leading to single-pixel-sized spikes in the images (Law et al. 2006b, 2009). The images with diffraction limited core size ($\sim 0.15''$) were assigned to the high-performance group, with smaller cores assigned to lower-performance groups.

Using a companion-detection simulation with a group of representative targets, we determine the angular separation and contrast consistent with a 5σ detection. For clarity, the contrast curves of the simulated targets are fitted with functions of the form $a - b/(r - c)$ (where r is the radius from the target star and a , b , and c are fitting variables). Contrast curves for the three performance groups are shown in Section 4.

3.1.4. Contrast Ratios

For wide companions, the binaries' contrast ratio was determined using aperture photometry on the original images. The aperture size was determined uniquely for each system based on separation and the presence of non-associated background stars.

For close companions, the estimated PSF was used to remove the blended contributions of each star before aperture photometry was performed. The locally optimized PSF subtraction algorithm attempts to remove the flux from companions using other reference PSFs with excess brightness

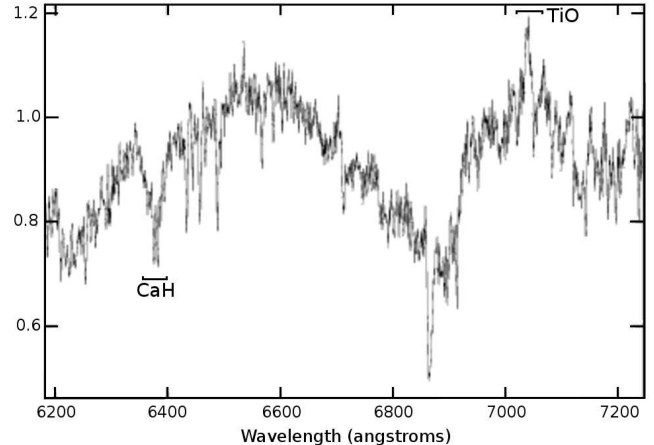


Figure 4. The extracted spectra for NLTT52532 showing subdwarf characteristics, most apparent the weakness of the 7050ÅTiO band and strength of the 6380ÅCaH band. The y-axis is given in normalized arbitrary flux units.

Table 2
Full SOAR Spectroscopic Observation List

NLTT	m_v	ObsID	Companion?
2205	14.0	2014 Jul 14	yes
7301	14.9	2014 Jul 14	yes
7914	14.3	2014 Jul 14	yes
9597	12.0	2014 Jul 14	
9898	14.2	2014 Jul 14	
10022	15.8	2014 Jul 14	
10135	15.7	2014 Jul 14	
33971	12.8	2014 Jul 14	
37342	14.4	2014 Jul 14	yes
37807	12.0	2014 Jul 14	
40022	13.9	2014 Jul 14	
40313	13.7	2014 Jul 14	
41111	13.7	2014 Jul 14	
44039	11.5	2014 Jul 14	
44568	12.3	2014 Jul 14	
49486	16.0	2014 Jul 14	yes
50869	15.8	2014 Jul 14	
52377	14.5	2014 Jul 14	yes
52532	15.5	2014 Jul 14	yes
53255	15.0	2014 Jul 14	yes
55603	12.1	2014 Jul 14	yes
56818	14.0	2014 Jul 14	yes
57038	13.9	2014 Jul 14	yes
58812	14.9	2014 Jul 14	yes

in those areas. For detection purposes, we use many PSF core sizes for optimization, and the algorithm's ability to remove the companion light is reduced. However, the companion is artificially faint as some flux has still been subtracted. To avoid this, the PSF fit was redone excluding a six-pixel-diameter region around the detected companion. The large PSF regions allow the excess light from the primary star to be removed, while not reducing the brightness of the companion.

3.1.5. Separation and Position Angles

Separation angles were determined from the raw pixel positions. Uncertainties were found using estimated systematic errors due to blending between components. Typical uncertainty in the position for each star was 1-2 pixels. Position angles were calculated using a distortion solution produced using Robo-AO measurements for a globular cluster.⁴

⁴ S. Hildebrandt (2013, private communication).

3.2. Previously Detected Binaries

To further realize our goal of a comprehensive cool subdwarf survey, we included in our statistics previously confirmed binary systems in the literature with separations outside of our field of view. Common proper motion is a useful indicator of wider binary systems. Wide ($>30''$) common proper motion companions among our target subdwarfs were previously identified in the Revised New Luyten Two-Tenths (rNLTT) catalog (Salim & Gould 2002; Chanamé & Gould 2004), and a search by López et al. (2012) of the Lepine and Shara Proper Motion-North catalog (Lépine & Shara 2005).

The target list was also cross-checked against the *Ninth Catalogue of Spectroscopic Binary Orbits* (Pourbaix et al. 2004, S_B^9), a catalogue of known spectroscopic binaries available online.⁵ While these systems were included in the total subdwarf binary numbers, the compilatory nature of this catalogue leaves some uncertainty in the completeness of the spectroscopic search.

3.3. Spectroscopy

To further verify that the targets selected are cool subdwarfs, we took spectra of 7% of the total survey and 31% of the candidate companion systems. Past spectroscopic studies of cool subdwarfs at high resolution have proven difficult as, at the low temperatures present, a forest of molecular absorption lines conceals most atomic lines used in spectral analysis. Subdwarfs can be classified spectroscopically using two molecular lines (Gizis 1997). Comparing titanium oxide (TiO) bands to metal hydride bands (typically CaH in M subdwarfs), Gizis classified two groups, the intermediate and extreme subdwarfs. As the metallicity decreases, the TiO adsorption also decreases, but the CaH remains largely unaffected for a given spectral type. This classification system was expanded and revised to include ultra subdwarfs by Lépine et al. (2007), who introduced the new useful parameter $\zeta_{\text{TiO}/\text{CaH}}$.

Spectra were taken for wavelengths 5900-7400Å, and reduced (dark-subtracted and flat-fielded) using IRAF reduction packages, particularly the onedspec.apall to extract the trace of the spectrum and onedspec.dispcor for applying the wavelength calibration. A Fe+Ar arc lamp was recorded for wavelength calibration. All observed target subdwarfs were confirmed to show the spectral characteristics of subdwarf stars described above, specifically the reduced band strength of 7050ÅTiO5. An example of the extracted spectra is given in Figure 4. The full observation list for SOAR is given in Table 2.

3.4. Candidate Companion Follow-ups

With either high contrast ratio or small angular separation, six candidate subdwarf binary systems with low detection significance ($<6\sigma$) were selected for follow-up imaging using Keck II. One low-probability candidate companion star was rejected after followups using Keck II, an apparent close ($\rho \approx 0.15''$) binary to NLTT50869, probably resulting from a cosmic ray on the original Robo-AO image. A wider binary to NLTT50869, with high detection significance, was not in the image field of view. Outside of the six target stars with low significant companions, another candidate companion star, NLTT4817, was observed and had no companion inside the field of view of the Keck II image, however had a

Table 3
Full Keck-AO Observation List

NLTT	m_v	ObsID	Low-sig. Companion?
4817	11.4	2014 Aug 17	
7914	14.3	2014 Aug 17	yes
50869	15.8	2014 Aug 17	
52377	14.5	2014 Aug 17	yes
52532	15.5	2014 Aug 17	yes
53255	15.0	2014 Aug 17	yes
56818	14.0	2014 Aug 17	yes

high significant companion ($>7\sigma$) in the Robo-AO field of view. An example of the Keck II images and the Robo-AO images is given in Figure 5. The full Keck II observations are listed in Table 3, with the last column indicating the presence of the low detection significance companion.

4. DISCOVERIES

Of the 344 verified subdwarf targets observed, 40 appear to be in multiple star systems for an apparent binary fraction of $11.6\% \pm 1.8\%$, where the error is based on Poissonian statistics (Burgasser et al. 2003). This count includes 6 multiple systems first recorded in the NLTT, 13 systems first recorded in the rNLTT, 1 wide binary found in the LSPM (López et al. 2012), 6 spectroscopic binaries, and 16 newly discovered multiple systems. We also found four new companions to already recorded binary systems, including two new triple systems, for a total of 6 triple star systems, for a triplet fraction of $1.7\% \pm .7\%$. One quarter (26%) of the companions would only be observable in a high-resolution survey ($<2.0''$ sep). The binary fraction of the target stars binned by their $(V-J)$ color is given in Figure 6. Cutouts of the closest 22 multiple star systems are shown in Figure 8. Measured companion properties are detailed in Table 4.

4.1. Probability of Association

The associations of all discovered and previously recorded companions were confirmed using the Digitized Sky Survey (DSS) (Reid et al. 1991). Since all the targets have high proper motions, if not physically associated the systems would have highly apparent shifts in separation and position angle over the past two decades. For the widely separated systems with both stars visible in the DSS, we checked the angular separation in the DSS and our survey to confirm relatively constant separation. For closely separated systems where both stars are merged in the DSS, we looked for a background star at the DSS position that does not appear in our images.

In addition, since our stars appear in relatively sparse stellar regions in the sky, well outside the Galactic disk, the probability of a background star appearing in a close radius to our observed star is low. Using the total number of known non-associated stars in our images, than we expect over all target stars in our survey 1.2 background stars within a radius of $2''.5$ of any of our target stars, compared to 10 stars observed in that range.

4.2. Photometric Parallaxes

Very few subdwarfs in our sample have accurate parallax measurements. Only 43 of the targets have published parallaxes, most with significant measurement errors. To estimate the distances to our subdwarf targets, we employed an expression for $M_R = f(R-I)$ estimated by Siegel et al. (2002) using a

⁵ <http://sb9.astro.ulb.ac.be/>

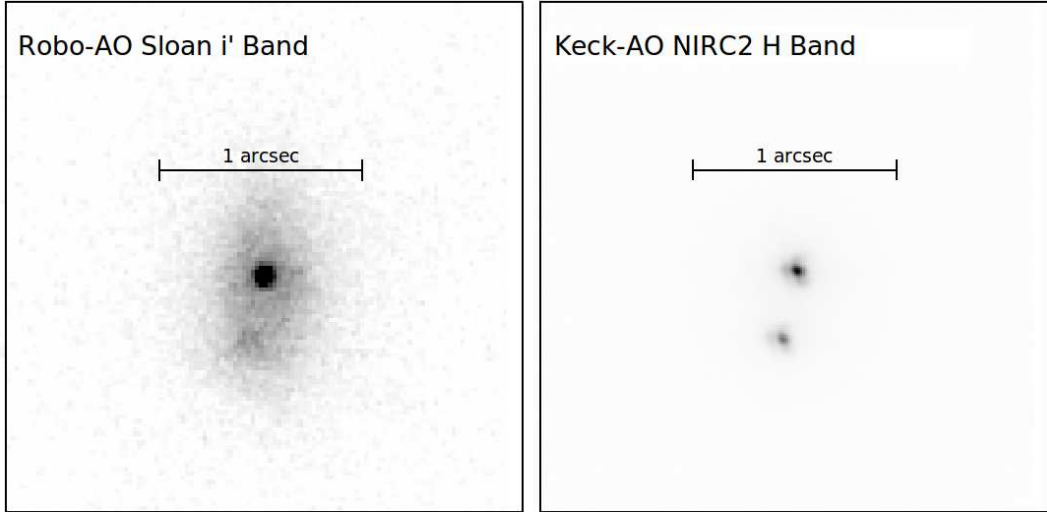


Figure 5. Keck-AO confirming the Robo-AO companion to NLTT52532. Exposure time for the Robo-AO image is 120 s and for the Keck-AO image is 90 s.

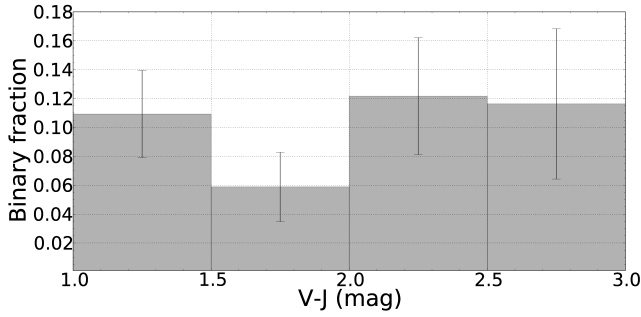


Figure 6. Binary fraction of the target subdwarfs binned by their $(V - J)$ color.

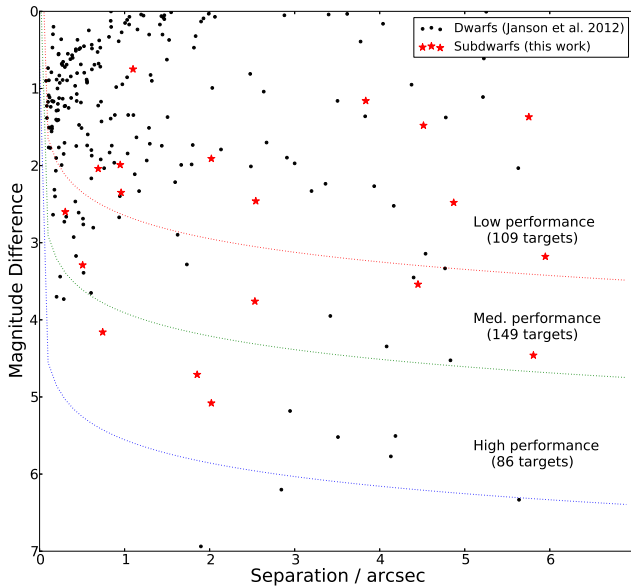


Figure 7. Comparison of the separation and the magnitude difference in the i -band between our subdwarf companions ($<6''$) and the dwarf companions found by Janson et al. (2012). The detectable magnitude ratios for our image performance groups are also plotted, with the number of observed subdwarfs targets in each image performance group, as described in Section 3.1.3.

color-magnitude diagram and the photometric measurements by Marshall (2007).

The polynomial fit found by Siegel for subdwarfs with measured parallaxes and an estimated mean $[Fe/H]$ of -1.2 , and with the Lutz & Kelker (1973) correction, is

$$M_R = 2.03 + 10 \times (R - I) - 2.21 \times (R - I)^2 \quad (3)$$

The color-absolute magnitude relation has an uncertainty of ~ 0.3 mag. In all cases, the published parallax errors are much larger than photometric errors of <0.03 mag. The estimated distances for the primary stars in the subdwarf multiple systems are listed in Table 4.

5. DISCUSSION

5.1. Comparison to Main-Sequence Dwarfs

With comparable sample size and spectrum types, the cool dwarf survey of Janson et al. (2012) is a useful metal-rich analog to this work. The most striking disparity between the two samples is the lack of low-contrast ($\Delta m_i \leq 2$), close ($\rho \leq 1''$) companions to the subdwarf stars, a regime heavily populated by solar-metallicity dwarf companions. This is clearly seen in a plot of the companion's magnitude difference versus angular separation for the two populations, as in Figure 7.

The dissimilarity between contrast ratios between dwarfs and subdwarfs is further illustrated in Figure 9. A two sample Kolmogorov-Smirnov test rejects the null hypothesis that the two populations are similar at a confidence of $\sim 2.8\sigma$.

The lack of close subdwarf companions has been noted previously by Jao et al. (2009) and by Abt (2008), however with significantly smaller samples. A direct comparison of orbital separations is biased by the relative distance variation in the two samples. With their relative rarity in the solar neighborhood, the subdwarf sample is overall approximately a factor of 4 further distant than the dwarf sample. If the populations were similar, this would result in a relative abundance of tight dwarf binaries, while the $6''$ limit of the Janson et al. survey reduces the number of observed wide dwarf binaries. Attempts to pick out similar systems by relative distance or by orbital separation from the two surveys results in a small statistical sample. Nonetheless, the relative lack of close stars in the subdwarfs sample, as illustrated in Figure 10, and confirmed at high-confidence in our survey, warrants further investigation.

Table 4
Multiple subdwarf systems resolved using Robo-AO and previously detected systems

NLTT	Comp NLTT	m_v^a (mag)	ObsID	$\Delta i'$ (mag)	ρ (")	ρ (AU)	P.A. (deg.)	Dist (pc)	Prev Det?
2045AB	...	13.5	2013 Aug 15	183.3±21.0	SB9
2205AB	2206	13.9	2013 Aug 15	0.18	3.37	475.5±54.3	123±2	140.9±16.1	L79
2324AB	2325	15.7	2013 Aug 16	1.16	3.84	138.8±15.9	254±2	36.1±4.1	L79
2324AC	...	15.7	2013 Aug 16	4.14	23.48	847.8±96.2	159±2	36.1±4.1	
4817AB	4814	11.4	2012 Sep 3	4.30	24.59	3615±413	218±2	147±16.8	S02
7301AB	7300	14.9	2012 Sep 3	2.48	4.87	105.7±12.1	57±2	21.7±2.5	S02
7914AB	...	14.3	2012 Sep 3	3.76	2.53	424.4±48.5	150±2	167.6±19.2	
10536AB	10548	11.2	2013 Aug 15	...	185.7	30633±3501	85.5	164.9±18.9	S02
11015AB	11016	16.3	2013 Aug 16	0.94	9.24	1399±160	57±2	151.3±17.3	S02
12845AB	...	10.6	2012 Oct 3	4.71	1.85	149.4±17.1	92±2	80.6±9.2	
15973AB	15974	9.3	2012 Oct 7	3.47	6.88	303.1±34.6	227±2	44±5.0	S02
15973AC	...	9.3	2012 Oct 7	5.02	8.23	362.2±41.1	217±2	44±5.0	
17485AB	...	11.9	2012 Oct 10	191.3±21.9	SB9
18502AB	...	12.2	2013 Jan 19	3.18	5.95	1262±144	331±2	212.1±24.3	
18798AB	18799	14.5	2013 Jan 19	3.12	12.82	2270±259	172±2	177±20.2	S02
19210AB	19207	11.2	2013 Jan 20		102.5	18468±2110	285.4	180.2±20.6	S02,SB9
20691AB	...	9.6	2013 Jan 19	70.6±8.1	SB9
21370AB	...	13.7	2013 Jan 19	2.46	19.83	6603±755	322±2	332.9±38.1	SB9
24082AB	...	13.1	2013 Jan 19	4.46	5.81	1683±192	187±2	289.7±33.1	
24082AC	...	13.1	2013 Jan 19	4.17	12.00	3476±397	267±2	289.7±33.1	
25234AB	25233	13.2	2013 Jan 18	3.05	8.29	1175±134	287±2	141.7±16.2	S02
28434AB	...	14.9	2013 Jan 17	2.46	2.54	652.9±74.6	202±2	256.7±29.3	
29551AB	...	11.5	2012 Sep 3	3.29	0.51	104.6±12.0	355±2	206.5±23.6	
29594AB	...	13.2	2013 Apr 22	...	38.10	12834±1466	269	336.8±38.5	L12
30193AB	...	14.6	2013 Apr 21	1.99	0.95	304.8±34.8	304±2	321.5±36.7	
30838AB	30837	12.5	2013 Apr 22	5.69	16.25	4436±507	25±2	273±31.2	S02
31240AB	...	15.0	2013 Apr 21	4.16	0.74	251.2±28.7	210±2	338.3±38.7	
31240AC	...	15.0	2013 Apr 21	3.86	10.32	3491±399	157±2	338.3±38.7	
34051AB	...	13.5	2013 Jan 19	242.3±27.7	SB9
37342AB	37341	14.4	2013 Apr 22	1.37	5.75	123.4±14.1	54±2	21.4±2.5	S02
45616AB	...	11.9	2012 Sep 3	2.59	28.31	4696±536.8	113±2	165.9±19.0	SB9
49486AB	49487	15.9	2012 Oct 4	1.48	4.51	390.3±44.6	148±2	86.4±9.9	S02
49819AB	49821	14.0	2013 Aug 19	1.12	25.28	10263±1173	84±2	406±46.4	S02
50759AB	50751	15.9	2012 Sep 13	...	297.7	79156±9046	267.7	265.8±30.4	S02
50869AB	...	15.8	2013 Aug 8	3.15	8.17	1707±195	19±2	209.0±24.0	
52377AB	...	14.5	2012 Sep 4	2.35	0.92	561.3±64.2	211±2	585.3±66.9	
52532AB	...	15.5	2012 Sep 4	2.60	0.30	52.82±6.0	168±2	175±20.0	
52532AC	52538	15.5	2012 Sep 4	3.35	37.14	6536±780	...	176±21.0	L79
53255AB	...	15.0	2013 Aug 16	0.75	1.07	123.9±14.2	68±2	112.7±12.9	
53255AC	53254	15.0	2013 Aug 16	...	53.8	6063±694	...	112.7±12.9	L79
55603AB	...	12.1	2013 Aug 18	3.54	4.45	886.9±101.4	29±2	199.2±22.8	
56818AB	...	14.0	2012 Sep 3	2.04	0.63	169.8±19.4	44±2	246.2±28.1	
57038AB	...	13.9	2013 Aug 16	0.19	8.14	2508±286.7	335±2	308.3±35.2	
57452AB	...	13.6	2013 Aug 16	1.91	1.98	474.5±54.2	77±2	234.9±26.9	
57856AB	...	13.2	2013 Aug 17	5.08	2.00	585.3±66.9	169±2	289.7±33.1	
58812AB	58813	15.0	2013 Aug 16	1.40	2.81	743.6±85.0	69±2	264.4±30.2	

Notes. — References for previous detections are denoted using the following codes: Pourbaix et al. 2004 (SB9); Luyten 1979 (L79); Samir et al. 2002 (S02); López et al. 2012 (L12).

^a(Marshall 2007)

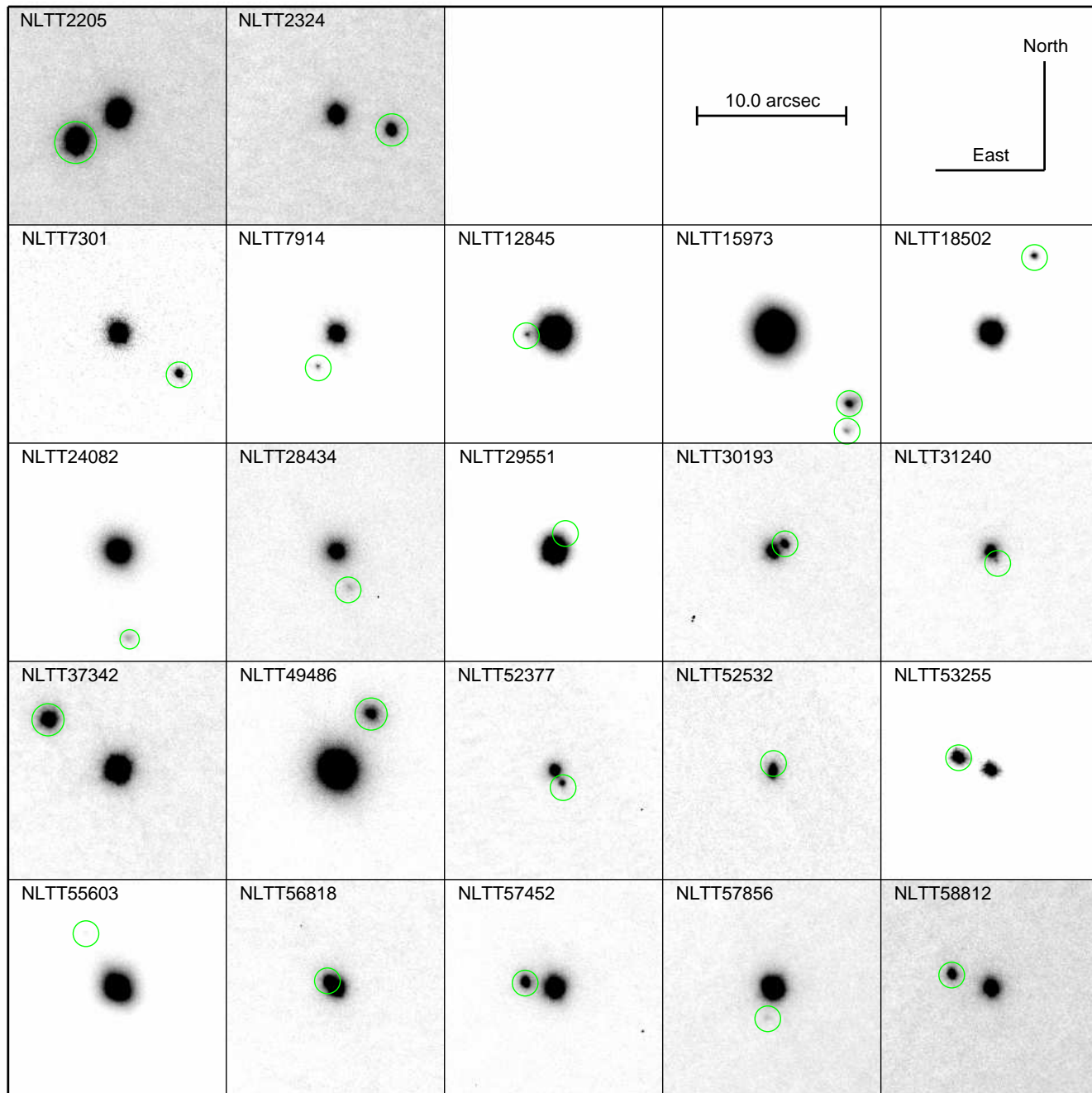


Figure 8. Gray scale cutouts of the 22 multiple star systems with separations $<7''$ resolved with Robo-AO. The angular scale and orientation is similar for each cutout.

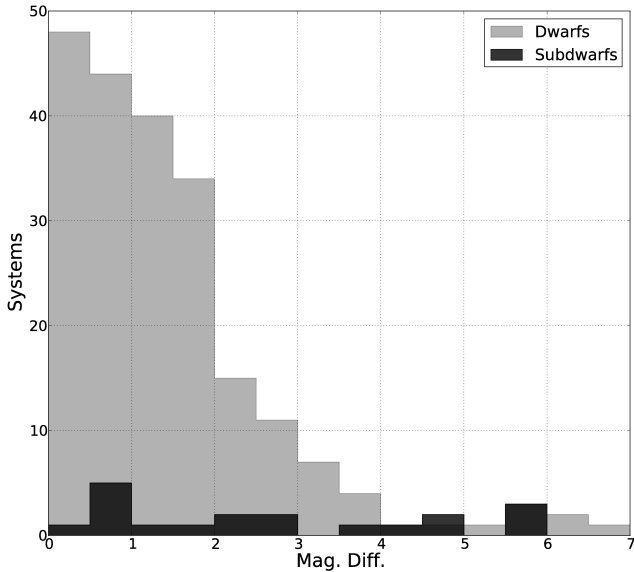


Figure 9. Histogram of the magnitude difference in the *i*-band between all our subdwarf companions and the dwarf companions found by Janson et al. (2012).

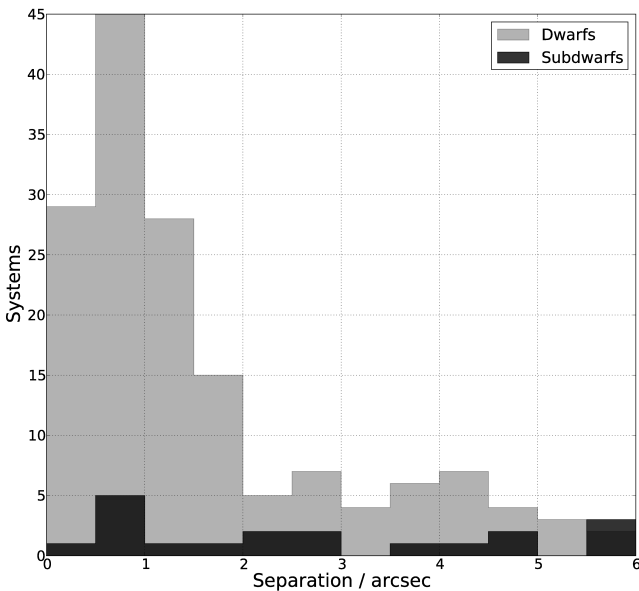


Figure 10. Histogram of the angular separations of our subdwarf companions and the dwarf companions found by Janson et al. (2012). Only systems resolvable in both surveys were plotted ($0'.15 < \rho < 6'.0$)

5.2. Binarity and Metallicity

The binary fraction we have found further confirms what has been suspected by past studies: that the binary fraction of subdwarfs is substantially lower than their dwarf cousins. The largest survey of cool subdwarfs, although limited by the low angular resolution of the SDSS, Zhang et al. (2013), find a multiplicity for type late K and M subdwarfs of 2.41%, with an estimated lower bound of 10% when adjusting for survey incompleteness. This estimate and our work leave subdwarfs multiplicity rates approximately a factor of 2 to 4 lower than solar-metallicity stars of the same spectral types.

Historically, it has been a widely held view that metal-poor stars possess fewer stellar companions (Batten 1973; Latham 2004). A deficiency of eclipsing binaries was found in globu-

lar clusters by Kopal (1959), while Jaschek & Jaschek (1959) discovered a deficiency of spectroscopic binaries in a sample of high-velocity dwarfs. Abt & Willmarth (1987) used higher resolution CCD spectra to conclude that the frequency of spectroscopic binaries in high-velocity stars was half of metal-rich stars. Recently, however, this view has come under attack. Carney et al. (1994) used radial velocity measurements of 1464 stars, along with metallicity data (Carney et al. 1987), and found the difference in binary frequency of metal-rich and metal-poor stars to not be significant. Likewise, Grether & Lineweaver (2007) found a $\sim 2\sigma$ anti-correlation between metallicity and companion stars.

In recent years, the relationship between planetary systems and metallicity has also been explored. Fischer & Valenti (2004) found a positive correlation between planetary systems and the metallicity of the host star. This correlation has been reinforced to $\sim 4\sigma$ by Grether & Lineweaver (2007). Recently, Wang et al. (2014) found that planets in multiple-star systems occur 4.5 ± 3.2 , 2.6 ± 1.0 , and 1.7 ± 0.5 times less frequently when the companion star is separated by 10, 100, and 1000 AU, respectively.

The solution may lie in the differences between halo and thick disk stars. Latham et al. (2002) found no obvious difference between the binary fraction of the two populations, however Chiba & Beers (2000) found a 55% multiplicity rate for thick disk stars and 12% for halo stars. Grether & Lineweaver also find that the thick disk shows a ~ 4 times higher binary fraction than halo stars, further hypothesizing that the mixing of the populations is the explanation for the perceived anti-correlation of metallicity and binarity.

The large difference between the M subdwarfs and thick-disk M dwarfs, apparent in our work in this paper and Janson et al. (2012), seems to imply the two populations formed under different initial conditions. Star formation in less dense regions appear to lower binary rates. Köhler et al. (2006) found a factor 3-5 difference in binary fraction between the low-density Taurus star-forming region and the dense Orion cluster. It is also possible that, as older than solar-abundance stars, the metal-poor subdwarfs could have suffered more disruptive encounters with other stars. These disturbances could separate companions with separations larger than a few AU, with the tighter, more highly bound systems being less affected (Sterzik & Durisen 1998; Abt 2008), a theory derived from *N*-body simulations (Aarseth & Hills 1972; Kroupa 1995). This, however, is contrary to our tentative result of a lack of close subdwarf companions, and the similar observations of Jao et al. (2009) and Abt (2008) that close subdwarf binaries are rare. This implies that metal-poor subdwarfs had shorter lifetimes in clusters than their younger, metal-rich cousins, either being ejected or formed in a disrupted cluster.

Another possible explanation is that a large number of low-metallicity stars in the Milky Way could have resulted from past mergers with satellite galaxies. Simulations from Abadi et al. (2006) predict that the early Galaxy underwent a period of active merging. From these mergers, the Galaxy would inherit large numbers of metal-poor stars. Meza et al. (2005) observe a group of metal-poor stars with angular momenta similar to the cluster ω Cen, long theorized to be the core of a dwarf galaxy that merged with the Milky Way. The environment of these foreign galaxies is unknown, so star formation could be quite different than our own Galaxy. It is also possible that during the merger multiple close stellar encounters and perturbations could alter their primordial binary

properties.

6. CONCLUSIONS

In the largest high-resolution binary survey of cool subdwarfs, we observed 344 stars with the Robo-AO robotic laser adaptive optics system, sensitive to companions at $\rho \geq 0''.15$ and $\Delta m_i \leq 6$. Of those targets, we observed 16 new multiple systems and 4 new companions to already known binary systems. When including previously recorded multiple systems, this implies a multiplicity rate for cool subdwarfs of $11.6\% \pm 1.8\%$ and a triplet fraction of $1.7\% \pm .7\%$. This is significantly lower than the observed cool subdwarf binarity of $26\% \pm 6\%$ by [Jao et al. \(2009\)](#) and in agreement with the completeness adjusted estimate of $> 10\%$ of [Zhang et al. \(2013\)](#). When comparing our results to similar surveys of dwarf binarity, we note a $\sim 2.8\sigma$ difference in relative magnitude differences between companions. An apparent lack of close binaries is noted, as has been previously observed in the literature. The high efficiency of Robo-AO makes large, high-angular resolution surveys practical and will in the future continue to put tighter constraints on the properties of stellar populations.

ACKNOWLEDGEMENTS

The Robo-AO system is supported by collaborating partner institutions, the California Institute of Technology and the Inter-University Centre for Astronomy and Astrophysics, and by the National Science Foundation under Grant Nos. AST-0906060, AST-0960343, and AST-1207891, by the Mount Cuba Astronomical Foundation, by a gift from Samuel Oschin.

We are grateful to the Palomar Observatory staff for their ongoing support of Robo-AO on the 60 inch telescope, particularly S. Kunsman, M. Doyle, J. Henning, R. Walters, G. Van Idsinga, B. Baker, K. Dunscombe and D. Roderick. The SOAR telescope is operated by the Association of Universities for Research in Astronomy, Inc., under a cooperative agreement between the CNPq, Brazil, the National Observatory for Optical Astronomy (NOAO), the University of North Carolina, and Michigan State University, USA. We also thank the SOAR operators, notably Sergio Pizarro. We recognize and acknowledge the very significant cultural role and reverence that the summit of Maunakea has always had within the indigenous Hawaiian community. We are most fortunate to have the opportunity to conduct observations from this mountain.

C.B. acknowledges support from the Alfred P. Sloan Foundation.

This research has made use of the SIMBAD database, operated by Centre des Données Stellaires (Strasbourg, France), and bibliographic references from the Astrophysics Data System maintained by SAO/NASA.

Facilities: PO:1.5m (Robo-AO), Keck:II (NIRC2-LGS), SOAR (Goodman)

7. APPENDIX

In Table 5, we list our Robo-AO observed subdwarfs, including date the target was observed, observation quality as described in Section Section 3.1.3, and the presence of detected companions.

Table 5 Full Robo-AO Observation List

NLTT	m_v	ObsID	Obs. qual	Companion?
69	15.2	2012 Oct 10	low	
193	15.5	2013 Aug 15	medium	
341	12.1	2012 Oct 10	high	
361	15.4	2013 Aug 17	low	
496	15.8	2012 Sep 04	medium	
660	15.7	2012 Sep 03	low	
812	12.8	2012 Sep 03	high	
933	15.5	2013 Aug 16	low	
1020	15.3	2013 Aug 15	medium	
1059	13.8	2012 Sep 04	medium	
1231	11.9	2013 Aug 16	high	
1509	15.8	2013 Aug 16	low	
1575	16.2	2012 Sep 03	low	
1635	13.2	2012 Sep 03	high	
1684	15.1	2012 Sep 13	low	
1815	15.5	2012 Sep 04	low	
1870	13.9	2012 Sep 03	medium	
2045	13.5	2013 Aug 15	medium	yes
2107	15.5	2012 Sep 04	low	
2205	14.0	2013 Aug 15	medium	yes
2324	15.7	2013 Aug 16	medium	yes
2868	13.5	2013 Aug 16	medium	
2953	15.9	2012 Sep 04	low	
2966	15.6	2012 Sep 04	medium	
3035	15.9	2012 Sep 04	low	
3965	16.1	2013 Aug 16	medium	
4245	15.6	2013 Aug 15	low	
4447	15.9	2012 Sep 03	low	
4817	11.4	2012 Sep 03	high	yes
4838	15.4	2012 Sep 03	low	
5022	13.9	2012 Sep 03	medium	
5192	14.3	2012 Sep 03	medium	
5289	15.6	2012 Sep 03	low	
6519	14.8	2012 Sep 03	medium	
6582	15.7	2013 Aug 17	low	
6614	15.7	2012 Sep 03	medium	
6816	16.1	2013 Aug 15	low	
6856	16.1	2012 Sep 03	low	
6863	15.3	2013 Aug 17	low	
7078	14.4	2012 Sep 03	medium	
7207	14.5	2013 Aug 15	medium	
7299	11.5	2013 Aug 16	high	
7301	14.9	2012 Sep 03	high	yes
7415	9.1	2012 Sep 03	high	
7417	11.6	2013 Aug 15	high	
7467	15.9	2012 Sep 13	low	
7596	16.2	2013 Aug 17	low	
7654	16.1	2013 Aug 16	medium	
7769	14.0	2012 Sep 03	medium	
7914	14.3	2012 Sep 03	medium	yes
8034	11.8	2012 Sep 03	high	
8227	10.5	2013 Aug 17	high	
8342	14.9	2012 Sep 03	medium	
8405	15.8	2012 Sep 03	medium	
8507	13.9	2012 Sep 03	medium	
8783	11.5	2012 Sep 03	high	
8866	15.8	2013 Aug 16	low	
9523	15.4	2013 Aug 15	low	
9550	15.5	2013 Aug 19	low	
9578	10.5	2013 Aug 15	high	
9597	12.0	2012 Sep 13	high	
9622	14.3	2012 Sep 04	medium	
9648	14.9	2012 Sep 04	medium	
9653	15.6	2013 Aug 16	low	
9727	15.8	2013 Aug 15	medium	
9734	15.0	2012 Sep 04	medium	
9799	15.4	2012 Sep 13	low	
9848	16.6	2013 Aug 19	low	
9898	14.2	2013 Aug 19	low	
9938	16.2	2013 Aug 15	low	
10018	15.4	2013 Aug 17	low	
10022	15.8	2013 Aug 16	medium	
10135	15.7	2012 Sep 04	low	
10176	15.8	2013 Aug 20	low	
10243	14.1	2012 Sep 04	medium	
10401	14.6	2013 Aug 18	low	
10517	14.5	2012 Sep 04	medium	

TABLE 5 – *Continued*

NLTT	m_v	ObsID	Obs. qual	Companion?
10536	11.2	2013 Aug 15	high	yes
10548	15.9	2013 Aug 15	low	
10850	10.7	2012 Sep 04	high	
10883	15.9	2012 Sep 04	low	
11007	12.2	2013 Aug 21	high	
11010	14.1	2012 Sep 04	medium	
11015	16.3	2013 Aug 16	low	yes
11032	14.2	2012 Sep 04	medium	
11068	15.4	2013 Aug 21	low	
11938	14.3	2012 Sep 04	medium	
12017	12.3	2013 Aug 17	high	
12026	15.8	2013 Aug 18	low	
12044	15.8	2012 Sep 13	low	
12227	14.2	2013 Aug 18	medium	
12350	12.1	2013 Aug 18	medium	
12489	14.6	2012 Oct 10	low	
12537	14.5	2013 Aug 21	medium	
12704	15.4	2012 Oct 10	low	
12769	14.1	2013 Aug 18	medium	
12829	14.6	2012 Oct 03	medium	
12845	10.6	2012 Oct 03	high	yes
12856	10.8	2013 Aug 18	high	
12876	15.6	2012 Oct 03	low	
12923	15.2	2013 Aug 18	low	
13022	15.9	2012 Oct 03	low	
13344	13.8	2012 Oct 03	medium	
13368	15.5	2012 Oct 03	low	
13402	14.7	2012 Oct 03	low	
13469	15.1	2013 Aug 18	low	
13470	13.8	2012 Oct 03	medium	
13641	12.9	2012 Oct 06	high	
13660	12.4	2012 Oct 03	high	
13694	15.4	2013 Aug 20	medium	
13706	14.5	2012 Oct 03	low	
13770	12.4	2012 Oct 03	high	
13811	13.4	2012 Oct 03	medium	
13920	14.4	2013 Aug 20	medium	
13940	14.4	2012 Oct 05	medium	
14091	13.9	2012 Oct 05	medium	
14131	13.4	2012 Oct 03	medium	
14169	13.4	2012 Oct 05	medium	
14197	12.4	2012 Oct 04	low	
14391	13.5	2012 Oct 04	low	
14450	14.7	2012 Oct 04	low	
14549	14.5	2012 Oct 10	low	
14822	12.7	2012 Oct 03	medium	
14864	14.3	2012 Oct 07	low	
15039	14.8	2012 Oct 10	low	
15183	12.6	2012 Oct 07	medium	
15218	12.3	2012 Oct 06	high	
15973	9.3	2012 Oct 07	high	yes
15974	13.8	2012 Oct 07	high	
16030	13.9	2012 Oct 07	low	
16185	14.4	2012 Oct 10	low	
16242	10.6	2012 Oct 06	medium	
16579	12.3	2012 Oct 09	high	
16606	12.3	2012 Oct 10	high	
16849	15.3	2012 Oct 10	low	
16869	13.2	2013 Jan 20	high	
16986	15.8	2013 Jan 20	low	
17039	12.9	2012 Oct 10	medium	
17485	11.9	2012 Oct 10	high	yes
17680	13.6	2013 Jan 20	medium	
17786	12.0	2013 Jan 20	high	
17872	10.7	2013 Jan 20	high	
18019	13.3	2012 Oct 10	medium	
18131	14.4	2013 Jan 20	medium	
18424	12.7	2013 Jan 18	high	
18463	13.8	2013 Jan 20	high	
18502	12.2	2013 Jan 19	high	yes
18731	13.1	2013 Jan 19	high	
18798	14.5	2013 Jan 19	high	yes
18799	11.0	2013 Jan 19	high	
19037	14.9	2013 Jan 20	medium	
19210	11.2	2013 Jan 20	high	yes
19301	14.7	2013 Jan 19	low	
19570	14.4	2013 Apr 22	medium	
19614	15.7	2013 Apr 22	medium	

TABLE 5 – *Continued*

NLTT	m_v	ObsID	Obs. qual	Companion?
19643	11.9	2013 Jan 19	high	
19824	14.6	2013 Jan 19	medium	
20252	14.9	2013 Apr 22	medium	
20288	14.9	2013 Apr 22	medium	
20392	13.8	2013 Jan 22	low	
20476	13.2	2013 Apr 22	high	
20492	13.3	2013 Jan 19	high	
20684	12.0	2013 Jan 19	high	
20691	9.6	2013 Jan 19	high	yes
20768	14.0	2013 Jan 19	medium	
21039	14.0	2013 Jan 19	medium	
21112	15.3	2013 Apr 22	medium	
21133	12.7	2013 Jan 19	medium	
21341	14.3	2013 Jan 19	low	
21370	13.7	2013 Jan 19	medium	yes
21449	12.6	2013 Apr 22	high	
21601	14.6	2013 Apr 22	medium	
22026	12.6	2013 Apr 22	high	
22053	12.1	2013 Jan 19	high	
22520	10.8	2013 Jan 19	high	
22752	13.9	2013 Jan 19	medium	
22945	13.2	2013 Apr 22	medium	
23894	14.6	2013 Jan 18	low	
24006	15.5	2013 Apr 22	medium	
24082	13.1	2013 Jan 19	medium	yes
24353	13.2	2013 Jan 18	medium	
24371	14.2	2013 Jan 18	low	
24718	13.1	2013 Jan 18	medium	
24984	12.5	2013 Apr 21	high	
25006	14.1	2013 Apr 21	medium	
25177	12.2	2013 Apr 22	high	
25190	13.9	2013 Jan 18	low	
25234	13.2	2013 Jan 18	medium	yes
25475	13.9	2013 Apr 21	medium	
25776	13.8	2013 Apr 22	medium	
25909	13.5	2013 Apr 22	high	
25970	14.9	2013 Jan 18	low	
26232	14.4	2013 Jan 18	low	
26482	12.5	2013 Jan 18	medium	
26503	14.2	2013 Apr 21	medium	
26532	14.8	2013 Jan 18	low	
26565	14.8	2013 Jan 18	low	
26588	13.6	2013 Apr 21	high	
26677	13.5	2013 Jan 18	low	
27436	13.0	2013 Jan 18	medium	
27763	13.6	2013 Jan 18	medium	
27767	14.7	2013 Apr 21	medium	
28199	13.2	2013 Jan 18	medium	
28304	13.3	2013 Apr 22	medium	
28434	14.9	2013 Jan 17	low	yes
29023	13.0	2013 Jan 18	medium	
29064	14.0	2013 Apr 21	medium	
29256	14.7	2013 Jan 18	low	
29442	14.4	2013 Jan 18	low	
29551	11.5	2013 Apr 21	high	yes
29594	13.2	2013 Apr 22	high	yes
29933	10.2	2013 Apr 22	high	
30128	13.1	2013 Apr 21	high	
30193	14.6	2013 Apr 21	medium	yes
30462	12.8	2013 Jan 18	medium	
30636	14.8	2013 Jan 18	low	
30824	14.6	2013 Jan 17	low	
30838	12.5	2013 Apr 22	high	yes
31146	12.0	2013 Apr 21	high	
31155	13.6	2013 Jan 18	medium	
31240	15.0	2013 Apr 21	medium	yes
31965	14.2	2013 Jan 19	medium	
32316	11.3	2013 Apr 22	high	
32392	14.6	2013 Jan 19	medium	
32562	14.3	2013 Jan 17	low	
32648	12.8	2013 Jan 18	medium	
32917	13.8	2013 Apr 22	medium	
32995	13.4	2013 Apr 22	high	
33104	14.0	2013 Jan 18	low	
33156	14.2	2013 Apr 22	medium	
33371	12.8	2013 Jan 17	medium	
33971	12.8	2013 Jan 18	medium	
34051	13.5	2013 Jan 19	low	yes

TABLE 5 – *Continued*

NLTT	m_v	ObsID	Obs. qual	Companion?
34628	11.9	2013 Apr 21	high	
35068	13.2	2013 Jan 18	medium	
35318	13.4	2013 Apr 21	high	
36020	14.2	2013 Apr 22	medium	
37342	14.4	2013 Apr 22	high	yes
37684	13.3	2013 Apr 22	high	
37807	12.0	2013 Apr 22	high	
39378	13.5	2013 Apr 22	high	
39721	13.6	2013 Apr 22	high	
40022	13.9	2013 Apr 22	medium	
40313	13.7	2013 Apr 22	high	
41111	13.7	2013 Apr 22	medium	
44039	11.5	2012 Sep 14	high	
44233	15.2	2012 Sep 04	low	
44568	12.3	2012 Sep 04	high	
44639	11.8	2012 Sep 04	high	
44769	15.2	2013 Apr 21	medium	
45609	12.5	2012 Sep 04	high	
45616	11.9	2012 Sep 04	high	yes
47480	13.8	2012 Oct 05	low	
47543	9.2	2012 Oct 05	medium	
48011	14.7	2012 Oct 05	high	
48056	13.7	2012 Oct 07	low	
48391	15.2	2012 Oct 05	medium	
48592	12.2	2012 Oct 04	medium	
48866	12.7	2012 Oct 04	medium	
49486	16.0	2012 Oct 04	medium	yes
49487	12.3	2012 Oct 04	medium	
49488	14.9	2013 Aug 19	medium	
49618	12.2	2012 Oct 04	medium	
49726	15.9	2013 Aug 19	low	
49749	14.8	2012 Oct 03	medium	
49819	14.0	2013 Aug 19	high	yes
49821	12.8	2013 Aug 19	high	
49897	15.8	2012 Oct 04	low	
50257	13.8	2013 Aug 18	low	
50376	13.9	2012 Sep 13	medium	
50556	15.7	2012 Sep 13	low	
50759	15.9	2012 Sep 13	low	yes
50869	15.8	2013 Aug 19	low	
50911	11.6	2012 Sep 13	high	
51006	14.1	2013 Aug 19	medium	
51153	15.1	2012 Sep 13	low	
51740	15.3	2012 Sep 13	low	
51754	15.0	2012 Sep 13	low	
51824	11.9	2013 Aug 18	medium	
51856	13.4	2012 Sep 04	medium	
52089	14.9	2012 Sep 04	medium	
52377	14.5	2012 Sep 04	medium	yes
52532	15.5	2012 Sep 04	low	yes
52573	15.3	2013 Aug 18	low	
52666	15.0	2013 Aug 19	low	
52816	15.7	2012 Sep 13	low	
52894	16.0	2012 Sep 13	low	
53190	15.4	2013 Aug 16	medium	
53254	14.7	2013 Aug 16	medium	
53255	15.0	2013 Aug 16	medium	yes
53274	11.9	2013 Aug 17	high	
53316	15.4	2012 Sep 13	low	
53346	13.8	2013 Aug 17	medium	
53480	12.6	2013 Aug 17	high	
53702	15.3	2012 Sep 13	medium	
53707	12.1	2013 Aug 18	medium	
53781	13.8	2013 Aug 17	medium	
53801	11.8	2012 Sep 13	high	
53823	13.8	2013 Aug 18	low	
54027	13.3	2013 Aug 19	medium	
54088	14.1	2013 Aug 18	low	
54168	13.4	2013 Aug 17	medium	
54184	14.0	2013 Aug 17	medium	
54349	14.4	2012 Sep 13	medium	
54450	15.6	2013 Aug 16	low	
54578	15.8	2013 Aug 18	low	
54608	16.0	2013 Aug 16	low	
54620	15.2	2013 Aug 17	medium	
54699	15.1	2012 Sep 13	low	
54710	15.2	2012 Sep 13	low	
54730	11.5	2012 Sep 13	high	

TABLE 5 – *Continued*

NLTT	m_v	ObsID	Obs. qual	Companion?
55411	15.9	2013 Aug 16	low	
55603	12.1	2013 Aug 18	medium	yes
55732	13.4	2013 Aug 17	medium	
55733	14.5	2012 Sep 03	medium	
55942	13.5	2013 Aug 16	medium	
56002	14.4	2012 Sep 03	medium	
56290	12.6	2013 Aug 16	high	
56420	15.6	2012 Sep 03	low	
56533	15.9	2013 Aug 16	low	
56534	12.7	2013 Aug 17	high	
56774	12.9	2013 Aug 18	low	
56817	16.1	2013 Aug 17	low	
56818	14.0	2012 Sep 03	medium	yes
56855	13.7	2013 Aug 16	medium	
57038	13.9	2013 Aug 16	medium	yes
57214	15.8	2013 Aug 16	low	
57452	13.6	2013 Aug 16	medium	yes
57546	16.2	2013 Aug 17	low	
57564	10.6	2013 Aug 17	high	
57630	15.0	2013 Aug 16	medium	
57631	13.5	2013 Aug 17	medium	
57647	14.7	2013 Aug 17	medium	
57741	14.2	2013 Aug 17	medium	
57744	16.1	2013 Aug 17	low	
57781	10.1	2013 Aug 16	high	
57832	15.2	2012 Sep 03	medium	
57851	15.2	2012 Sep 03	medium	
57856	13.2	2013 Aug 17	medium	yes
58071	13.1	2012 Sep 03	medium	
58141	15.8	2013 Aug 16	low	
58403	15.2	2013 Aug 16	low	
58522	15.0	2013 Aug 17	medium	
58555	15.1	2012 Sep 03	medium	
58812	14.9	2013 Aug 16	medium	yes

REFERENCES

- Aarseth, S. L., & Hills, J. G. 1972, *A&A*, 21, 255
 Abadi, M. G., Navarro, J. F., Stenmetz, M. 2006, *MNRAS*, 365, 747
 Abt, H. A. 2008, *AJ*, 135, 722
 Abt, H. A., & Willmarth, D. W. 1987, *ApJ*, 318, 786
 Adams, W. S. 1915, *AJ*, 42, 187
 Baranec, C., Riddle, R., Law, N. M., et al. 2013, *J. Visualized Exp.*, 72, e50021
 Baranec, C., Riddle, R., Law, N.M., et al. 2014, *ApJ*, 790, L8
 Basu, S., & Vorobyov, E. I. 2012, *ApJ*, 750, 30
 Batten, A. H., 1973, *Binary and multiple systems of stars* (Oxford: Pergamon)
 Bourke, T. L., Myers, P. C., Evans, N. J., II., et al. 2006, *ApJ*, 649, L37
 Burgasser, A. J., Kirkpatrick, J. D., Reid, I. N., et al. 2003, *ApJ*, 586, 512
 Carney, B. W., Laird, J. B., Latham, D. W., & Kurucz, R. L. 1987, *AJ*, 94, 1066
 Carney, B. W., Latham, D. W., Laird, J. B., & Anguilar, L. A. 1994, *AJ*, 107, 2240
 Chabrier, G., Baraffe, I., Allard, F., & Hauschildt, P. 2000, *ApJ*, 542, 464
 Chanamé, J., & Gould, A. 2004, *ApJ*, 601, 289
 Chiba, M., & Beers, T. C. 2000, *ApJ*, 119, 2843
 Clemens, J. C., Crain, J. A., Anderson, R. 2004, *Proc. SPIE*, 5492, 331
 Duquennoy, A., & Mayor, M. 1991, *A&A*, 248, 485
 Fischer, D. A., & Marcy, G. 1992, *ApJ*, 396, 178
 Fischer, D. A., & Valenti, J. 2005, *ApJ*, 622, 1102
 Fruchter, A.S., & Hook, R. N. 2002, *PASP*, 114, 144
 Gizis, J. E. 1997, *AJ*, 113, 806
 Gizis, J., Reid, I. N. 2000, *PASP*, 112, 610
 Goodwin, S. P., Kroupa, P., Goodman, A., & Burkert, A. 2007, in *Protostars and Planets V*, ed. B. Reipurth, D. Jewitt, & K. Kiel (Tucson, AZ: Univ. Arizona Press), 133
 Goodwin, S. P., & Whitworth, A. 2007, *A&A*, 466, 943
 Gould, A., & Salim, S. 2003, *ApJ*, 582, 1001
 Grether, D., & Lineweaver, C. H. 2007, *ApJ*, 669, 1220
 Janson, M., Hormuth, F., Bergfors, C., et al. 2012, *ApJ*, 754, 44

- Janson, M., Bergfors, C., Brandner, W., et al. 2014, *ApJS*, 214, 17
- Jao, W.-C., Mason, B. D., Hartkopf, W.I., et al. 2009, *AJ*, 137, 3800
- Jaschek, C., & Jaschek, M. 1959, *Zt. F. Ap.*, 48, 263
- Kaltenegger, L., & Traub, W. A. 2009, *ApJ*, 609, 519
- Köhler, R., Petr-Gotzens, M. G., McCaughrean, M. J., et al. 2006, *A&A*, 458, 461
- Kopal, Z. 1959, *Close Binary Systems* (New York: Wiley), 7
- Kroupa, P. 1995, *MNRAS*, 277, 1491
- Kuiper, G. P. 1939, *ApJ*, 89, 548
- Lafrenière, D., Marois, C., Doyon, R., Nadeau, D., & Artigau, É. 2007, *ApJ*, 660, 770
- Latham, D.W., 2004, *ASP Conference Series Vol 318*, eds. Hilditch, R.W., Hensberge, H. & Pavlovski, K.
- Latham, D. W., Stefanik, R. P., Torres, G., et al. 2002, *ApJ*, 124, 1144
- Law, N. M., Hodgkin, S. T., Mackay, & C. D. 2006b, *MNRAS*, 368, 1917
- Law, N. M., Kraus, A. L., Street, R., et al. 2012, *ApJ*, 757, 133
- Law, N. M., Mackay, C. D., & Baldwin, J. E. 2006a, *A&A*, 446, 739
- Law, N. M., Mackay, C. D., Dekany, R. G., et al. 2009, *ApJ*, 692, 924
- Law, N. M., Morton, T., Baranec, C., et al. 2014, *ApJ*, 791, 35
- Lépine, S., Shara, M., 2005, *AJ*, 129, 1483
- Lépine, S., Rich, R. M., Shara, M. M. 2007, *ApJ*, 669, 1235
- Lodieu N., Zapatero Osorio M. R., Martín, E. L. 2009, *A&A*, 499, 729
- López, C. E., Calandra, F., Chalela, M., et al. 2012, *JDSO*, 8, 78
- Lutz, T. E., & Kelker, D. H. 1973, *PASP*, 85, 573
- Luyten, W. J. 1979b, *New Luyten Catalogue of Stars with Proper Motions Larger than Two-Tenths of an Arcsecond* (Minneapolis: Univ. Minnesota Press)
- Luyten, W. J., & Hughes, H. S. 1980, *Proper-Motion Survey with the Forty-Eight Inch Schmidt Telescope. LV. First Supplement to the NLTT Catalogue* (Minneapolis: Univ. Minnesota Press)
- Marshall, J. L. 2007, *AJ*, 134, 778
- Marshall, J. L. 2008, *AJ*, 135, 1000
- Meza, A., Navarro, J. F., Abadi, M. G., Stenmetz, M. 2005, *MNRAS*, 359, 93
- Monteiro, H., Jao, W.-C., Henry, T., et al. 2006, *ApJ*, 638, 446
- Peter, D., Feldt, M., Henning, T., & Hormuth, F. 2012, *A&A*, 538, 74
- Pourbaix, d., Tokovinin, A. A., Batten, A., H., et al. 2004, *A&A*, 424, 727
- Raghavan, D., McAlister, H. A., Henry, T. J., et al. 2010, *ApJS*, 190, 1
- Reid, I. N., Brewer, C., Brucato, R. J., & et al. 1991, *PASP*, 103, 661
- Reid, I. N., & Hawley, S. L. 2005, *New light on dark stars: red dwarfs, low-mass stars, brown dwarfs* (1st ed.; Chichester, UK: Praxis)
- Riaz, B., Gizis, J., Samaddar, D. 2008, *ApJ*, 672, 1153
- Riddle, R. L., Burse, M. P., Law, N. M., et al. 2012, *Proc. SPIE*, 8447, 84472O
- Salim, S., & Gould, A. 2002, *ApJ*, 575, L83
- Siegel, M. H., Majewski, S. R., Reid, I. N., Thompson, I. B. 2002, *ApJ*, 578, 151
- Sterzik, M. F., Durisen, R. H. 1998, *A&A*, 339, 95
- Stryker, L. L., Hesser, J. E., Hill, G., et al. 1985, *PASP*, 97, 247
- Thies, I., & Kroupa, P. 2007, *ApJ*, 671, 767
- Sandage, A., & Eggen, O. 1959, *MNRAS*, 119, 278
- van Dam, M., Bouchez, A., Le Mignant, D. et al. 2006, *ASP Conference Series*, 118, 310
- Wang, J., Fischer, D. A., Xie, J.-W., Ciardi, D. R. 2014, *ApJ*, 792, 111
- Wizinowich, P., Le Mignant, D., Bouchez, A. et al. 2006, *ASP Conference Series*, 118, 297
- York, D. G., Adelman, J., Anderson, J. E., et al. 2000, *AJ*, 120, 1579
- Zhang, Z. H., Pinfield, D. J., Burningham, B., et al. 2013, *MNRAS*, 434, 1005